Int. J. Electrochem. Sci., 17 **(2022)** Article Number: 220531, doi: 10.20964/2022.05.20

International Journal of
ELECTROCHEMICAL
SCIENCE
www.electrochemsci.org

Short Communication

Enhanced Corrosion Resistance of hot-dip Galvanized Zinc Coating on AZ31 Magnesium Alloy with Cu Interlayer

Yanqi Wang[1,*], *Guowei Liang*[2], *Jun Long*[1], *Xiaowei Feng*[1]

[1] Institute of New Materials, Guangdong Academy of Sciences, Guangzhou, Guangdong, 510651, China
[2] School of Material Science and Engineering, South China University of Technology, Guangzhou, Guangdong 510640, China
[*]E-mail: yale_w@163.com

Received: 2 February 2022 / *Accepted:* 27 February 2022 / *Published:* 5 April 2022

In this work, a galvanized zinc coating with a Cu interlayer was successfully coated onto AZ31 magnesium alloy. The microstructure and corrosion resistance of the zinc-coated magnesium alloy were then investigated using scanning electron microscopy (SEM), energy dispersive spectroscopy (EDS), optical microscopy (OM), electrochemical impedance spectroscopy (EIS), and potentiodynamic polarization testing. The results revealed that a dense pure zinc coating with a thickness of approximately 100 μm was coated on the magnesium alloy surface. A reaction/diffusion layer formed at the interface between the Cu interlayer and the magnesium alloy, implying that the bond between the galvanized zinc coating and the magnesium alloy was metallurgical. Electrochemical tests in a NaCl solution revealed that surface modification of the magnesium alloy with the zinc coating could significantly enhance the corrosion resistance of the magnesium alloy. In addition, the galvanic corrosion between the galvanized zinc coating and the magnesium alloy was also investigated and discussed.

Keywords: Magnesium alloy; Galvanized zinc coating; Surface treatment; Corrosion

1. INTRODUCTION

Magnesium alloys have excellent performance, e.g., low density, high specific strength and rigidity, good damping performance, electromagnetic shielding and radiation resistance. Thus, magnesium and its alloys have attracted increasing attention and possess great application potential in the automobile, aviation, electronics and military industries[1, 2]. However, due to the insufficient surface properties of magnesium alloys, their application is greatly restricted mainly due to poor corrosion resistance [2]. Surface technology, such as spraying[3, 4], laser and ion beam[5-7], physical/chemical vapor deposition[8], chemical conversion[9-13], electroplating/electroless

plating[14-16], anodic oxidation[17] and thermal diffusion[16, 18], have been used to improve the corrosion resistance of magnesium alloys. These protective coatings on magnesium alloys prepared by the abovementioned surface techniques include inorganic, organic, metal and mixed coatings[3, 12, 17, 19-25].

From the perspective of economy and practicality, metal and its alloy coatings, such as electroplating copper and electroless nickel[26-28], spraying aluminum/stainless steel/zinc coating[29-33], and thermal diffusion aluminum/zinc coating[18, 34], are generally used to enhance the corrosion resistance of magnesium alloys. In particular, metal coatings can not only provide a protective barrier for magnesium alloys in service environments but also ensure good electrical and thermal conductivity of magnesium alloy components. These advantages of metal coatings have attracted the attention of a large number of researchers. Zinc coatings often show excellent corrosion resistance in atmospheric and humid environments. The corrosion products of zinc coatings are also highly dense, which delays further corrosion[35, 36]. In addition, when compared with nickel, copper, stainless steel, titanium and other metal coatings, the potential difference between zinc coatings and magnesium alloys is relatively small, which helps to reduce the galvanic corrosion tendency between zinc coatings and magnesium alloys. Therefore, zinc coating is a relatively ideal metal coating to improve the corrosion resistance of magnesium alloys.

Cold/thermal spraying and thermal diffusion have been reported for the preparation of zinc-based coatings on magnesium alloys[4, 18, 29]. However, cold/thermally sprayed zinc coatings usually have pores and cracks, which cannot completely mimic the properties of the bulk metals. The heat treatment of a thermal diffusion zinc coating often requires a long time (100 minutes to more than 10 hours[18]), which means that the production efficiency is low. In addition, it is easy to cause a temperature increase in the process of zinc coating preparation, which reduces the microstructure and properties of the magnesium alloy. Note that the galvanized zinc coating possesses metallurgical bonding with the steel substrate, and it can be obtained in a very short time at a relatively low temperature[35-37]. Keeping this in mind, in this work, a hot-dip galvanized zinc coating with a Cu interlayer was developed on AZ31 magnesium alloy to enhance the corrosion resistance of the magnesium alloy. The corrosion behavior of the galvanized coating on the magnesium alloy was investigated. The interfacial reaction behavior between the Cu interlayer and the zinc bath, as well as the Cu interlayer and the magnesium alloy, was also investigated and discussed. In addition, the effect of the hot-dipping process on the microstructure change of the magnesium alloy was also investigated and discussed.

2. MATERIALS AND METHODS

2.1 Electroplating treatment

AZ31 magnesium alloy with a composition of 2.71 wt.% Al, 0.19 wt.% Mn, 0.69 wt.% Zn, and balance Mg was selected as the substrate for this work. The AZ31 magnesium alloy was cut into plates (size: 50 mm × 20 mm × 5 mm.). The sample surface was sequentially polished with 200, 500 and 1000 grit silicon carbide paper. Then, the polished samples were ultrasonically cleaned in anhydrous ethanol,

rinsed with distilled water, and finally dried in cool air. The above-treated samples were subjected to alkaline degreasing, pickling, activation, zinc leaching and copper electroplating in sequence, as described previously[28].

2.2. Hot-dipped galvanizing

The precopper samples were rinsed with flowing tap water and then dipped in a flux bath (95 g/L $ZnCl_2$ + 150 g/L NH_4Cl) at 58 °C for 60 s. The flux-coated samples were dried at 120 °C for 100 s in a drying box and then subsequently galvanized in a pure zinc bath at 435 °C for 90 s. The zinc-coated sample was cooled with water immediately after being lifted from the zinc bath.

2.3. Coating characterization

The cross-sectional morphology and elemental composition of the galvanized zinc coating on the magnesium alloy surface were characterized by scanning electron microscopy (SEM) equipped with EDS (GeminiSEM300). The electrochemical corrosion behavior of the AZ31 magnesium alloy and the galvanized zinc coating were estimated by electrochemical measurements using an electrochemical workstation (Gamry Interface 1000E). A static 3.5 wt.% NaCl solution was used as the electrolyte, and the samples were mounted with epoxy resin with an exposed area S = 1 cm^2. A three-electrode cell with the specimen as the working electrode, platinum as the counter electrode, and a saturated calomel electrode as the reference electrode was constructed. EIS spectra were collected with a frequency range of 10^5 Hz -10^{-2} Hz and an amplitude of ±10 mV at open circuit potential. Potentiodynamic polarization curves were obtained in the corrosive solution at a scanning rate of 0.1 mV/s.

3. RESULTS AND DISCUSSION

3.1 Microstructure observation

Fig. 1 shows the cross-sectional SEM backscattered images of the Cu interlayer and the galvanized zinc coating. The thickness of the Cu interlayer is approximately 15 μm before hot-dip galvanization (see the bright layer in Fig. 1a). After hot-dip galvanizing, one can observe a zinc layer with a thickness of approximately 105 μm covering the surface of the Cu interlayer (see the bright layer in Fig. 1b). Fig. 1c shows a high-magnification image of the interface layer between the galvanized zinc coating and the AZ31 magnesium alloy substrate. The line scans of Zn, Cu, Mg and Al crossing the coating are also shown in Fig. 1c. In Fig. 1c, the line scanning result indicates that the galvanized zinc coating is composed of a pure zinc layer, a Cu-Zn intermetallic layer (see reaction layer I), a Cu interlayer and an obvious intermetallic layer between the AZ31 magnesium alloy substrate and the Cu interlayer (see reaction layer II). The Cu-Zn intermetallic layer has a thickness of approximately 3.5 μm. Moreover, one can see that the Cu-Zn intermetallic layer is denser than the Cu layer. The thickness of the Cu interlayer is approximately 8 μm after hot-dip galvanization. The intermetallic layer appearing between

the AZ31 magnesium alloy substrate and the Cu interlayer has a thickness of approximately 2 μm. This result implies that the Cu interlayer was partially dissolved in the zinc bath, during which the formation of the Cu-Zn intermetallic layer occurred. Furthermore, a reaction/diffusion layer was also formed between the Cu interlayer and the magnesium alloy substrate, which is very beneficial for improving the bonding force between the galvanized zinc coating and the magnesium alloy.

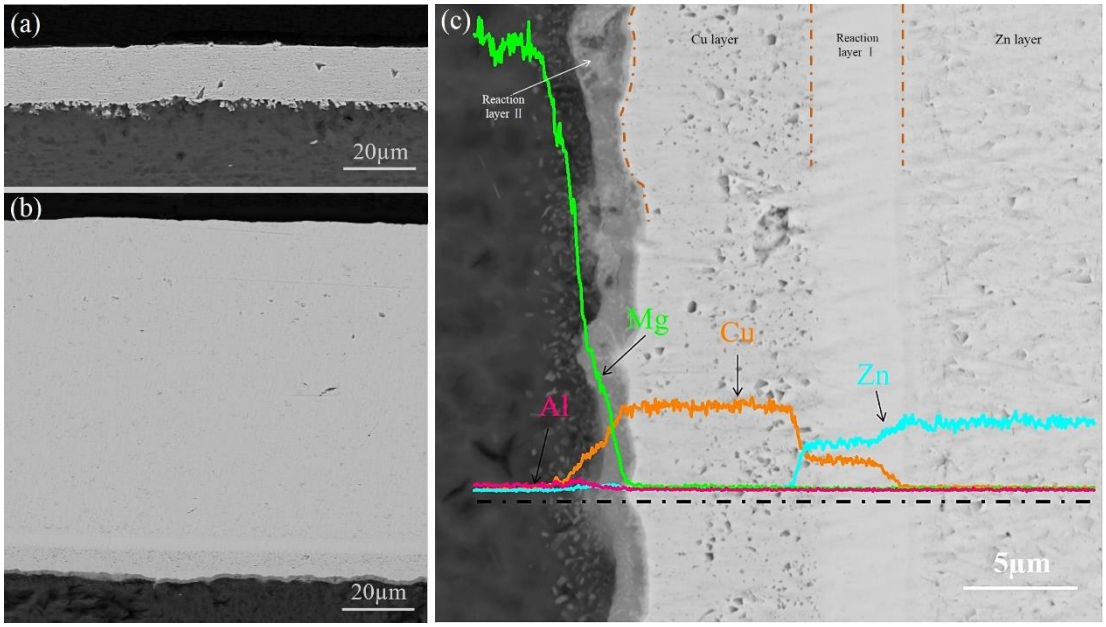

Figure 1. Cross-sectional SEM backscattered images of the coatings on the AZ31 magnesium alloy: a) Cu interlayer, b) galvanized zinc coating and c) high-magnification image of the interface layers between the galvanized zinc coating and the AZ31 magnesium alloy and its corresponding line scanning.

The interface layers between the AZ31 magnesium alloy substrate and the Cu interlayer before and after hot-dip galvanizing are presented in Fig. 2. One can see that the interface layers obtained before and after hot-dip galvanization are quite different. Fig. 2a shows that there is an obvious interface layer between the Cu interlayer and the AZ31 magnesium alloy. In Table 1, the EDS analysis result shows that there is a small amount of residual zinc layer between the Cu interlayer and the magnesium alloy. Note that the residual zinc layer should come from zinc leaching before Cu electroplating. Then, the Cu interlayer and the AZ31 magnesium alloy are basically in direct contact without a reaction layer. However, Fig. 2b shows that an obvious reaction/diffusion layer forms between the Cu interlayer and the AZ31 magnesium alloy, which indicates that a metallurgical bond is formed between the Cu interlayer and the AZ31 magnesium alloy after the hot-dipping process. Moreover, in Table 1, the EDS analysis result shows that the reaction/diffusion layer is mainly composed of Cu, Mg and Zn. In addition, in Fig. 2c-f, elemental maps also show that the interface layer between the Cu interlayer and the AZ31 magnesium alloy is mainly composed of Cu, Mg and Zn elements.

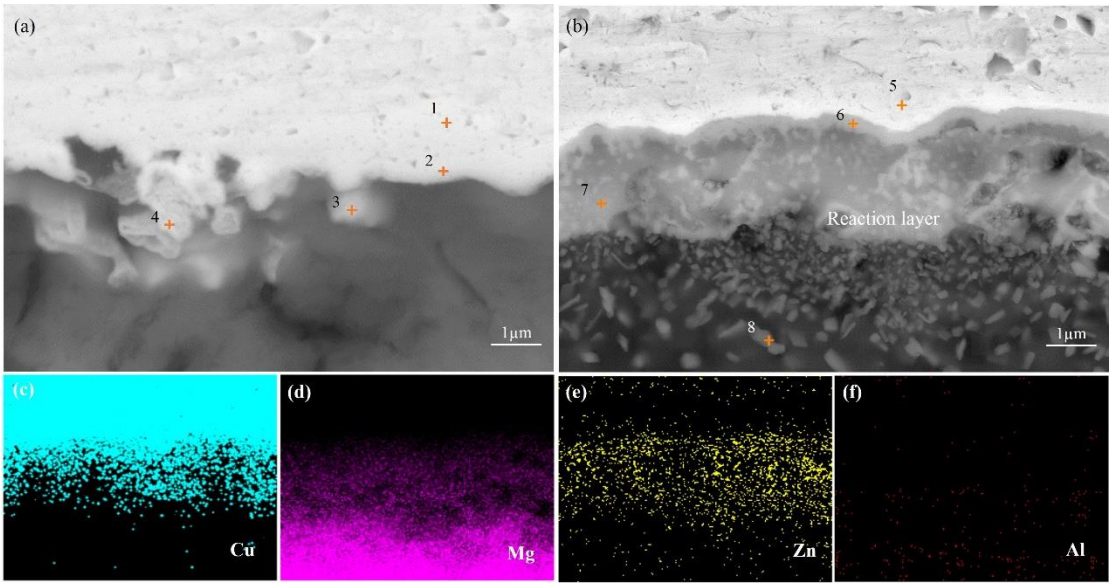

Figure 2. High-magnification image of the interface layers between the Cu interlayer and the AZ31 magnesium alloy: a) before hot-dip galvanization and b) after hot-dip galvanization and the corresponding elemental maps.

In Fig. 1, the microstructure observation indicates that a hot-dip galvanized zinc coating can be successfully developed on the AZ31 magnesium alloy with the Cu interlayer. According to the Mg-Zn binary phase diagram[38], one can see that the melting point of the Mg-Zn intermetallic compounds is lower than that of the zinc bath (approximately 435℃); the use of which would result in the failure to form a high melting point protective layer at the interface between the magnesium alloy and the zinc bath, and then the magnesium alloy would be quickly dissolved in the zinc bath. Therefore, in this paper, a high melting point Cu interlayer was preplated on the surface of the AZ31 magnesium alloy substrate (Fig. 1a). The Cu interlayer on the magnesium alloy surface serves two main functions: 1) prevents severe dissolution of the magnesium alloy in the acid pickling and fluxing solutions and 2) prevents the magnesium alloy from directly contacting the zinc bath, thereby avoiding rapid dissolution of the magnesium alloy in the zinc bath.

In Fig. 1a and c, one can see that the Cu interlayer is partially dissolved and that Cu-Zn intermetallic compounds form on the surface of the Cu interlayer. When the Cu interlayer contacts the zinc bath, it begins to dissolve, accompanied by the formation of the Zn-Cu intermetallic compound layer. The formation of the Zn-Cu intermetallic compound layer prevents the Cu interlayer from further rapid dissolution into the zinc bath. In Fig. 1c, the line scan results reveal that the Cu-Zn layer is a gradient metal layer with the zinc content gradually decreasing from the outside to the inside. According to the Zn-Cu binary phase diagram[39] and a previous study[40], the protective Zn-Cu layer may contain ε-$CuZn_5$, δ-$CuZn_3$, γ-Cu_5Zn_8 and β-CuZn phases from outside to inside crossing the galvanized zinc coating.

For the interface layer between the Cu interlayer and the magnesium alloy, the EDS analysis result (Fig. 2c-f and Table 1) reveals that the interlayer is mainly composed of Mg, Cu and Zn elements. During hot-dip galvanizing, the residual Zn layer (see Fig. 2a) derived from zinc leaching may melt and

react with the Cu interlayer and the magnesium alloy. The melted zinc may promote the mutual diffusion of magnesium and copper atoms, resulting in the formation of an obvious reaction/diffusion layer (see Fig. 2b). According to the Mg-Cu and Mg-Zn binary phase diagrams[38, 39, 41, 42], the reaction/diffusion layer may be composed of Mg-Cu, Mg-Zn, Cu-Zn and Mg-Zn-Cu intermetallic compounds. The formation of the reaction/diffusion layer is helpful to improve the bonding strength between the galvanized zinc coating and the magnesium alloy.

Fig. 3 shows the microstructure of the AZ31 magnesium alloy before and after hot-dip galvanization. In Fig. 3b, one can observe that the size, shape and distribution of the grains in the AZ31 magnesium alloy change very little when compared with the microstructure of the AZ31 magnesium alloy before hot-dip galvanization. However, in Fig. 3b, the occurrence of grain growth in some regions of the AZ31 magnesium alloy can still be observed (see the heat-affected zone). Grain growth occurs on the magnesium alloy substrate in the vicinity of approximately 500 μm from the zinc coating. This result reveals that the hot-dipping process can cause grain growth of the magnesium alloy. However, the region where grain growth occurred was not large since the hot dipping time (90 s) was very short. Therefore, the effect of the hot-dipping process on the physical properties of magnesium alloy should be limited.

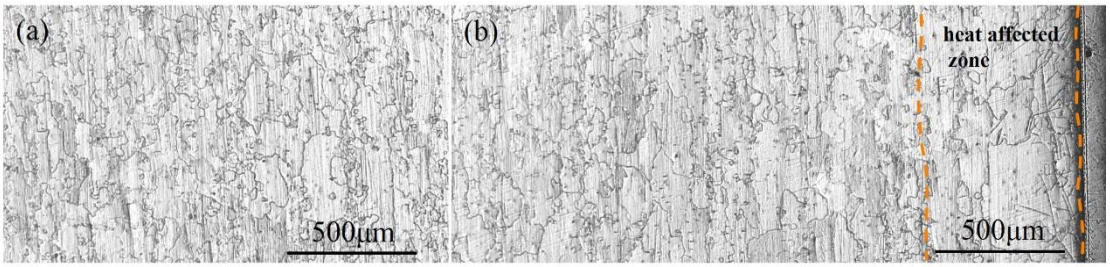

Figure 3. OM images showing the microstructure of the AZ31 magnesium alloy in this work: a) before hot-dip galvanization and b) after hot-dip galvanization.

3.2 Corrosion tests

3.2.1 Electrochemical corrosion behavior in a NaCl solution

The corrosion resistance of the galvanized zinc coating and the AZ31 magnesium alloy was comparatively investigated in a 3.5% NaCl solution. Fig. 4 shows the representative EIS spectra of the AZ31 magnesium alloy and the galvanized zinc coating. When observing the Nyquist diagram for the AZ31 magnesium alloy, it can be seen that the Nyquist diagram presents two loops with distinct features. In detail, at high frequencies, the Nyquist diagram presents a capacitance loop, and at low frequencies, it presents an inductive loop. The capacitance loop appears at high frequencies and could describe the charge transfer process of Mg/Mg^{2+} at the double layer between the magnesium surface and the electrolyte. The charge transfer resistance of the Mg electrode could be measured with the diameter of the capacitance loop[43]. For the inductive loop, it is generally believed that the inductive loop represents the desorption of corrosion products and the reaction of Mg^{+} with water[44]. For the Nyquist diagrams of the galvanized zinc coating, the Nyquist plot presents two distinct capacitive loops. The appearance of the first capacitive loop at high frequency is related to infiltration of the electrolyte; the existence of

the second capacitive loop at low frequency is attributed to charge transfer during the corrosion process and the behavior of the double layer at the coating/electrolyte interface[35].

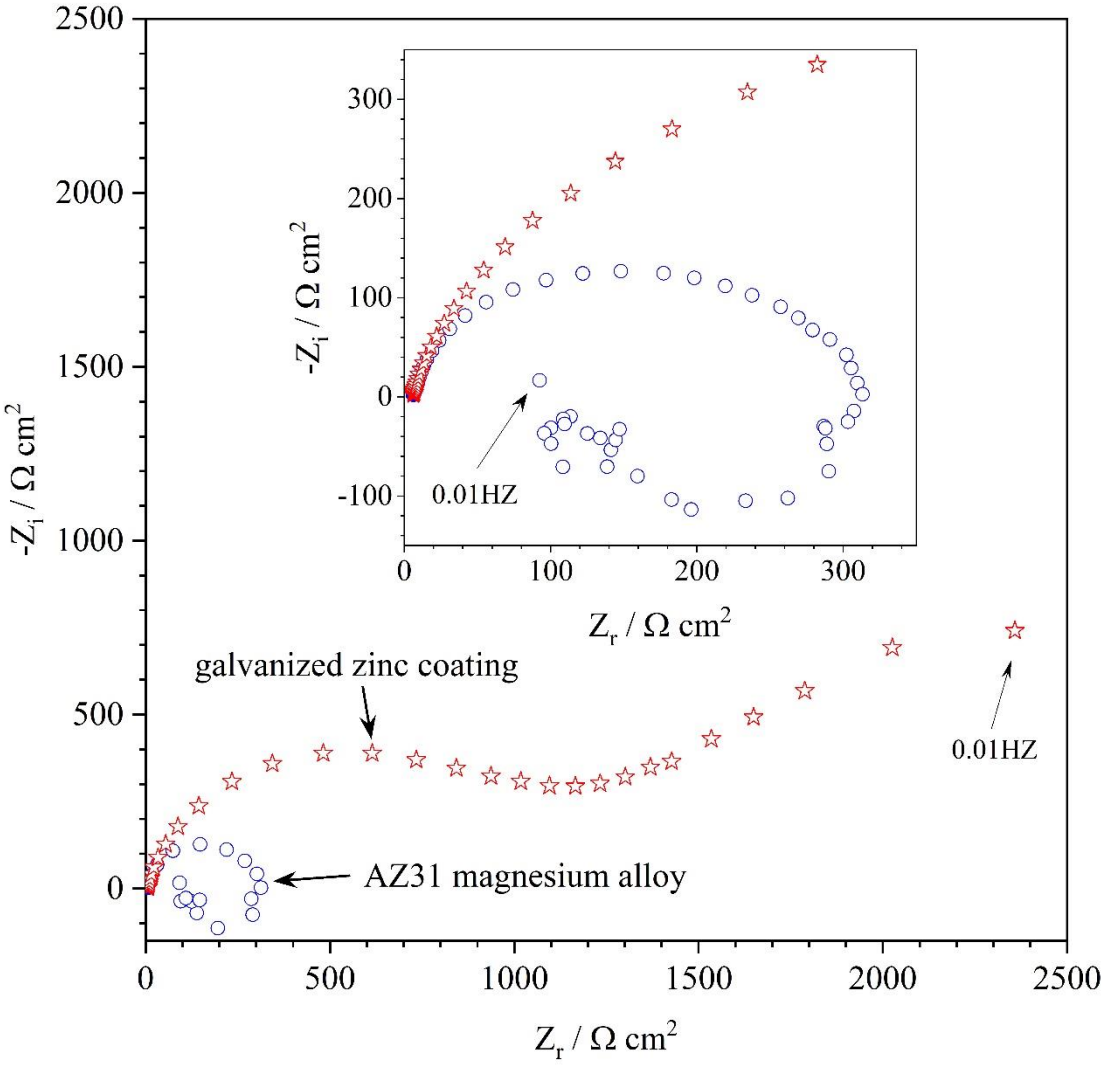

Figure 4. Representative EIS spectra of the AZ31 magnesium alloy and the galvanized zinc coating in a 3.5% NaCl solution.

Fig. 5 shows the equivalent circuit used to fit the EIS spectra of the samples. The calculated values are presented in Table 2. For the equivalent circuit for the AZ31 magnesium alloy in Fig. 5a, *Rs* was used to describe the solution resistance, and R_1 (the charge transfer resistance) and *CPE1* (constant phase element) were used to describe the properties of the capacitive loop at high frequency. Again, R_2 and *L* were used to describe the properties of the inductive loop at low frequency. Generally, the reciprocal of *Rp* (polarization resistance) is proportional to the corrosion resistance of the samples[43]. Based on the equivalent circuit model in Fig. 5a, the value of 1/*Rp* can be calculated by the following equation:

$$R_p = \frac{R_1 * R_2}{R_1 + R_2} \qquad (1)$$

For the equivalent circuit for the galvanized zinc coating in Fig. 5b, R_s was used to represent the solution resistance. The coating capacitance was represented by using a constant phase element CPE_1, and the coating resistance was described by using R_1. The double layer capacitance was described by using another constant phase element CPE_2, and the charge transfer resistance of the double layer was described by using R_2.

Because of the uneven distribution of the surface reactions, a *CPE* is usually used instead of a pure capacitance. The impedance of the *CPE* is calculated as follows:

$$Z_{CPE} = (Y_0)^{-1}(j\omega)^{-n} \qquad (2)$$

where Y_0, j, ω and n are defined as follows[35]:

Y_0 represents the initial admittance of the *CPE*, linking to the surface properties and the electroactive species;

J represents the imaginary unit, and $j^2 = -1$;

ω represents the angular frequency, and $\omega = 2\pi f$, where f is the frequency; and

n is the exponential term corresponding to the depression degree of the impedance spectra.

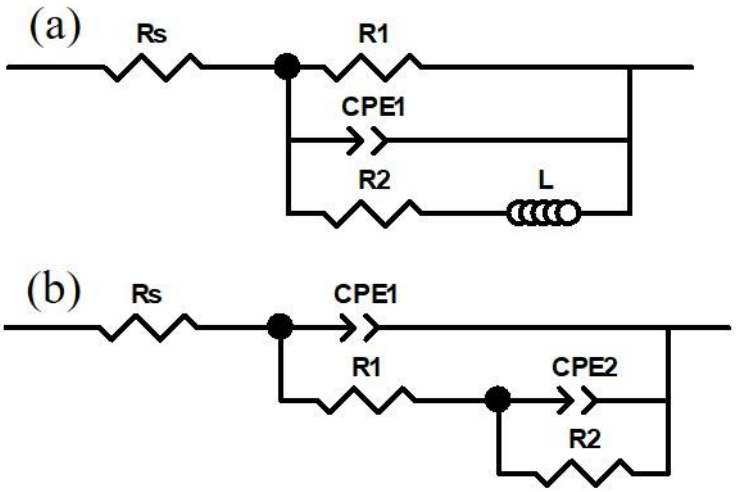

Figure 5. Equivalent electrical circuit used for the simulation of the EIS data: a) EEC model for the EIS data of the AZ31 magnesium alloy[41] and b) the EEC model for the EIS data of the galvanized zinc coating[32].

According to the fitting results in Table 2, one can observe that the obtained 1/*Rp* value of the galvanized zinc coating is obviously much smaller than that of the AZ31 magnesium alloy. This implies that the corrosion resistance of the AZ31 magnesium alloy can be dramatically improved by the galvanized zinc coating.

Fig. 6 presents the potentiodynamic polarization curves for the AZ31 magnesium alloy and the galvanized zinc coating. Table 3 lists the corresponding parameters obtained from the polarization curves in Fig. 6. In Fig. 6, one can observe that the experimental anodic Tafel regions of the two polarization curves are not well defined; then, the corrosion current density (i_{corr}) is determined by extrapolating the cathodic Tafel region[43]. As seen in Table 3, the corrosion potentials (E_{corr}) of the AZ31 magnesium

alloy and galvanized zinc coating are -1.56 V (vs. SCE) and -1.02 V (vs. SCE), respectively. After hot-dip galvanizing, the corrosion current density (i_{corr}) of the magnesium alloy significantly decreases from 79.35 μA/cm^2 to 3.83 μA/cm^2. The result is in good agreement with that obtained from the EIS study in Fig. 4.

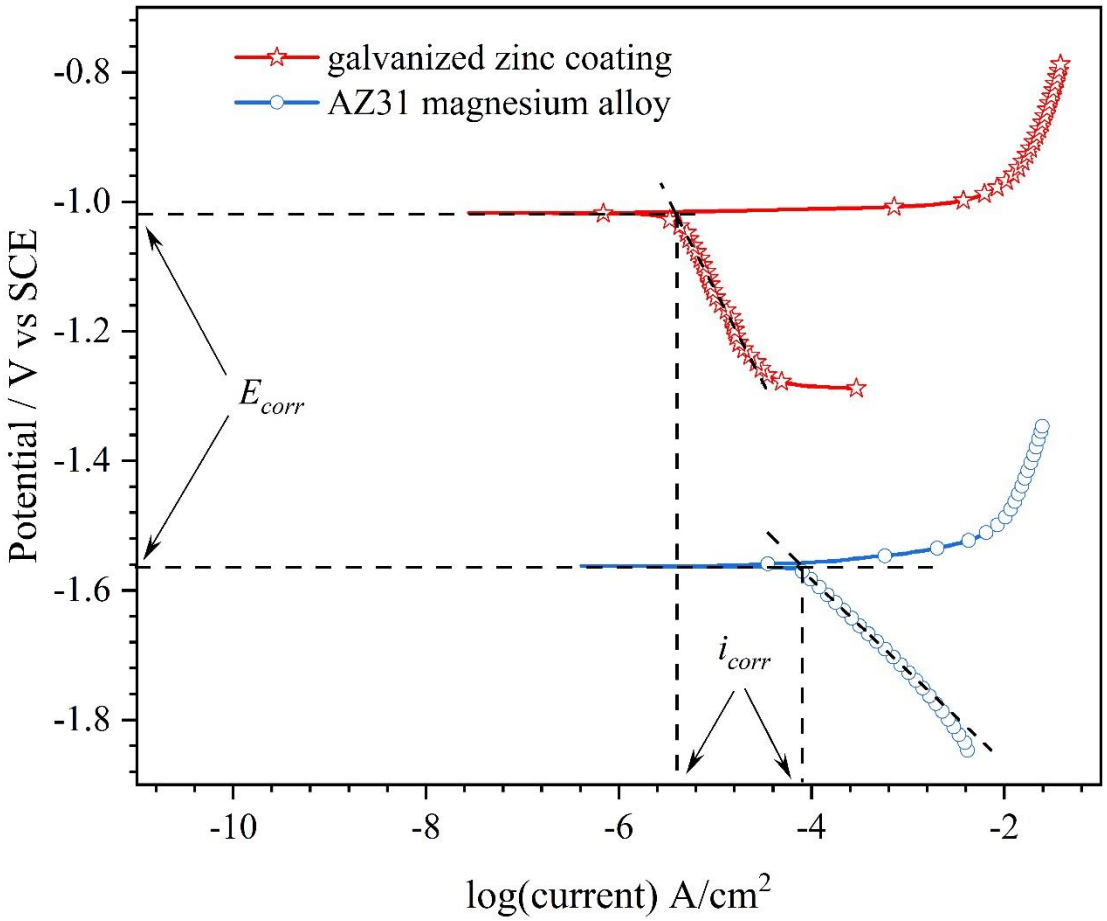

Figure 6. Representative polarization curves of the galvanized zinc coating and the AZ31 magnesium alloy in a 3.5% NaCl solution.

The results of the EIS and potentiodynamic polarization curves indicate that the corrosion resistance of the AZ31 magnesium alloy effectively improves after hot-dip galvanization. Since the galvanized zinc coating shows better corrosion resistance than the magnesium alloy in the NaCl solution, the magnesium alloy could be separated from the corrosive ions (such as Cl^-) by coating with a zinc layer. In addition, as the service life of the galvanized zinc coating is proportional to its thickness, it is necessary to cover the surface of the magnesium alloy with a thick galvanized zinc coating layer. Therefore, in this work, the galvanized zinc coating with a thickness of approximately 100 μm is very promising.

However, it should also be realized that since the corrosion potential of the zinc coating is higher than that of the magnesium alloy, once holes or cracks appear between the zinc layer and the magnesium

alloy, galvanic corrosion easily forms between the magnesium alloy and the zinc layer, which may accelerate the corrosion of the magnesium alloy. In conclusion, ensuring that the galvanized zinc coating has a certain thickness and integrity is very important to the improvement of the corrosion resistance of the magnesium alloy.

3.2.2 Cut-edge corrosion behavior in a NaCl solution

The galvanic corrosion behavior between the galvanized zinc coating and the AZ31 magnesium alloy was further investigated in a 3.5% NaCl solution. Fig. 7 shows the cut-edge corrosion morphology of the zinc-coated AZ31 magnesium alloy after 5 h of immersion. One can observe that corrosion occurs on the whole surface of the magnesium alloy, accompanied by the formation of obvious corrosion products. In addition, it can be seen that more corrosion products are formed on the surface of the magnesium alloy substrate near the zinc layer, implying that the corrosion degree of the magnesium alloy near the zinc layer may be more serious than that in other areas. For the galvanized zinc layer, its surface morphology is clearly visible (shown in Fig. 7b), and only a small amount of corrosion products appears on the surface of the galvanized zinc coating, which means that there is no corrosion or only slight corrosion occurring on the surface of the zinc layer. The map scan result indicates that the corrosion products are mainly composed of Mg and O elements, and some corrosion products containing Mg migrate to the zinc coating surface.

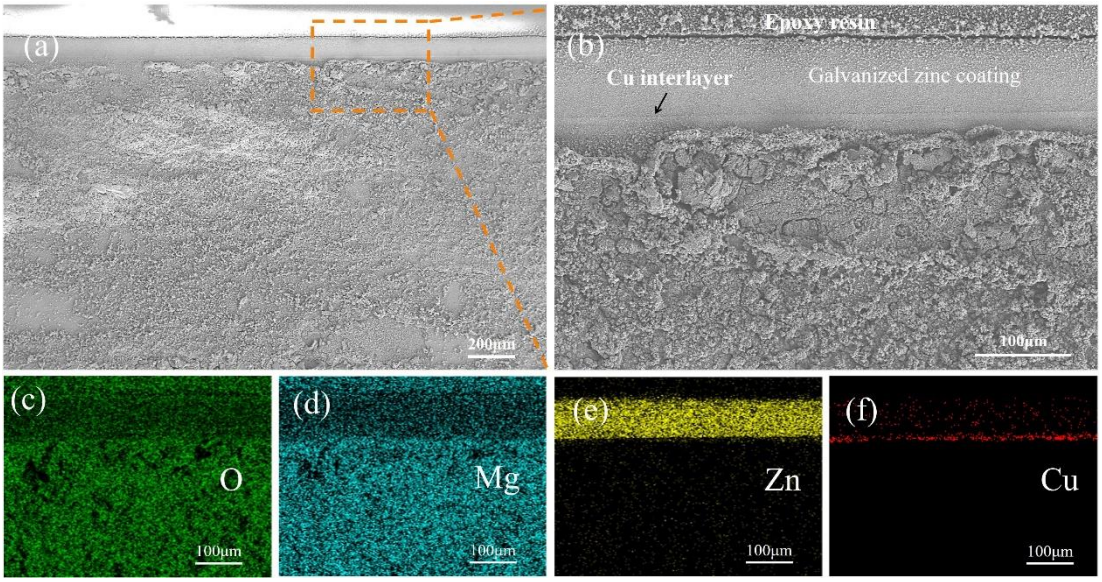

Figure 7. a) and b): SEM image of the corrosion morphology of the zinc-coated magnesium alloy in a 3.5% NaCl solution after 5 h of immersion and c)-f): the corresponding elemental maps.

Fig. 8 shows the corrosion morphology of the zinc-coated AZ31 magnesium alloy and the uncoated magnesium alloy after 24 h of immersion. In Fig. 8a, when compared with the corrosion morphology of the zinc-coated magnesium alloy, the corrosion degree of the magnesium alloy near the

zinc layer obviously increases, accompanied by the formation of significant corrosion pits and a large number of corrosion products. The surface morphology of the zinc coating is also clearly visible (shown in Fig. 8a), and only a small amount of corrosion products appears on the zinc coating surface. Fig. 8b shows that obvious corrosion pits appear on the surface of the uncoated magnesium alloy, accompanied by the formation of obvious corrosion products on the surface of the magnesium alloy. However, the width and depth of the corrosion pits on the surface of the magnesium alloy near the zinc coating are larger than those on the surface of the uncoated alloy. In conclusion, the galvanic corrosion between the zinc coating and the magnesium alloy induces obvious corrosion of the magnesium alloy.

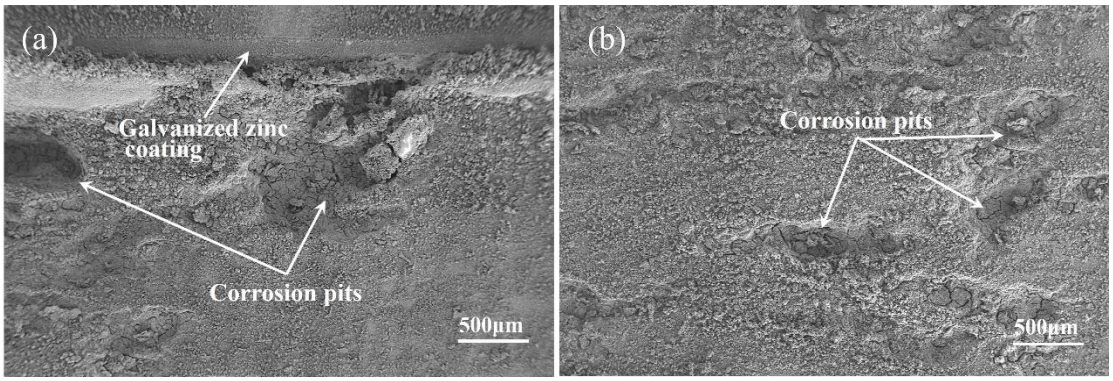

Figure 8. SEM image of the corrosion morphology of the magnesium alloy in a 3.5% NaCl solution after 24 h immersion for a) zinc-coated AZ31 magnesium alloy and b) uncoated AZ31 magnesium alloy.

The SEM morphology observation of the cut-edge corrosion behavior for the zinc-coated magnesium alloy in NaCl solution reveals that galvanic corrosion between the zinc coating and the magnesium alloy occurred, which increased the corrosion degree of the magnesium alloy near the galvanized zinc coating. In other words, it is very important to ensure the integrity of the galvanized zinc coating on the magnesium alloy surface. Otherwise, galvanic corrosion between the magnesium alloy and the zinc coating may aggravate the corrosion of the magnesium alloy substrate. The EIS study and potentiodynamic polarization curves in Figs. 4 and 6 reveal that the corrosion resistance of the galvanized zinc coating is significantly higher than that of the AZ31 magnesium alloy. Therefore, on the premise of ensuring the integrity of the galvanized zinc coating on the magnesium alloy, the galvanized zinc coating can not only provide good physical barrier protection for the magnesium alloy but also endow the magnesium alloy with good electrical and thermal conductivity.

4. CONCLUSIONS

A galvanized zinc coating was successfully developed on an AZ31 magnesium alloy using a hot-dipping method. This work may provide a new and relatively ideal method for the surface treatment of magnesium alloys with zinc coatings. The following conclusions can be drawn:

1. The introduction of the Cu interlayer on the magnesium alloy was an effective way to prevent the rapid dissolution of the magnesium alloy in the pickling solution, in the fluxing solution and in the zinc bath. Then, it is very important to ensure that the Cu interlayer is not completely dissolved during the hot-dipping process. Further study is also needed to understand the dissolution kinetics of the Cu interlayer in the zinc bath.
2. The galvanized zinc coating on the magnesium alloy had a thickness of approximately 100 μm. A reaction/diffusion layer could be formed at the interface between the Cu interlayer and the magnesium alloy, which is beneficial to improving the bonding strength between the zinc coating and the magnesium alloy.
3. The hot-dipping process exhibited a limited influence on the microstructure of the AZ31 magnesium alloy. Only a slight grain growth could be observed in the magnesium alloy in the vicinity of approximately 500 μm from the zinc coating.
4. The corrosion resistance of the zinc-coated magnesium alloy was significantly improved due to the high corrosion resistance of the zinc coating in a chloride-containing environment. However, it is worth noting that the corrosion degree of the magnesium alloy near the zinc coating increases due to the galvanic corrosion between the zinc coating and the magnesium alloy. Therefore, it is important to ensure the integrity of the galvanized zinc coating on the magnesium alloy.

DECLARATION OF COMPETING INTEREST

The authors declare that they have no known competing financial interests or personal relationships that could have appeared to influence the work reported in this paper.

ACKNOWLEDGMENTS

This work was supported by GDAS' Special Project of Science and Technology Development [2020GDASYL-20200103135].

References

1. Y. Yang, X. Xiong, J. Chen, X. Peng, D. Chen, F. Pan, *J. Magnesium Alloys*, 9 (2021) 705-747.
2. M. Esmaily, J.E. Svensson, S. Fajardo, N. Birbilis, G.S. Frankel, S. Virtanen, R. Arrabal, S. Thomas, L.G. Johansson, *Prog. Mater. Sci.,* 89 (2017) 92-193.
3. H.-L. Yao, Z.-H. Yi, C. Yao, M.-X. Zhang, H.-T. Wang, S.-B. Li, X.-B. Bai, Q.-Y. Chen, G.-C. Ji, *Ceram. Int.,* 46 (2020) 7687-7693.
4. K. Wang, S. Wang, T. Xiong, D. Wen, G. Wang, W. Liu, H. Du, *Surf. Coat. Technol*., 387 (2020) 125549.
5. S. Jana, M. Olszta, D. Edwards, M. Engelhard, A. Samanta, H. Ding, P. Murkute, O.B. Isgor, A. Rohatgi, *Corros. Sci*., 191 (2021) 109707.
6. F. Iranshahi, M.B. Nasiri, F.G. Warchomicka, C. Sommitsch, *J. Alloys Compd*., 8 (2020) 1314-1327.
7. Y. Wang, *Int. J. Electrochem. Sci*., (2019) 11465-11479.
8. V. R, S. G, R. Velusamy, S. Ramakrishna, *Surf. Coat. Technol*., 411 (2021) 126972.
9. J. Qi, Z. Ye, N. Gong, X. Qu, D. Mercier, J. Światowska, P. Skeldon, P. Marcus, *Corros. Sci.,* 186 (2021) 109459.
10. W. Zai, X. Zhang, Y. Su, H.C. Man, G. Li, J. Lian, *Surf. Coat. Technol*., 397 (2020) 125919.
11. Q. Liang, *Int. J. Electrochem. Sci*., (2021) 210647.
12. H. Yang, *Int. J. Electrochem. Sci*., (2020) 12203-12219.
13. D. Liu, *Int. J. Electrochem. Sci*., (2019) 1434-1450.

14. W. Shang, X. Zhan, Y. Wen, Y. Li, Z. Zhang, F. Wu, C. Wang, *Chem. Eng. Sci*., 207 (2019) 1299-1308.
15. X. Guan, H. Zhu, J. Shi, S. Wei, Z. Shao, X. Shen, *Surf. Eng*., 35 (2019) 906-912.
16. Y.-r. Zhou, S. Zhang, L.-l. Nie, Z.-j. Zhu, J.-q. Zhang, F.-h. Cao, J.-x. Zhang, *Trans. Nonferrous Met. Soc. China*, 26 (2016) 2976-2987.
17. H. Zhu, X. Li, X. Guan, Z. Shao, *Met. Mater. Int*., 27 (2021) 3975-3982.
18. H. Wang, B. Yu, W. Wang, G. Ren, W. Liang, J. Zhang, *J. Alloys Compd*., 582 (2014) 457-460.
19. H. Yuan, L. Zhang, L. Wu, S. Zhu, Y. Sun, S. Guan, *Mater. Lett.,* 289 (2021) 129389.
20. J. Wang, C. Jin, D. Mei, Y. Ding, L. Chang, S. Zhu, L. Wang, Y. Feng, S. Guan, *Surf. Eng.,* 37 (2021) 963-971.
21. N. Rahimi Roshan, H. Hassannejad, A. Nouri, *Surf. Eng.,* 37 (2021) 236-245.
22. Y. Qi, Z. Peng, L. Wang, J. Zhou, P. Wang, J. Liang, *Surf. Eng*., 37 (2021) 360-364.
23. W. Jiang, H. Jiang, G. Li, F. Guan, J. Zhu, Z. Fan, Microstructure, *Met. Mater. Int*., 27 (2021) 2977-2988.
24. S. Taşci, R.C. Özden, M. Anik, *Met. Mater. Int.,* 25 (2019) 313-323.
25. K. Cao, *Int. J. Electrochem. Sci*., (2021) 210328.
26. J. Liu, X. Wang, Z. Tian, M. Yuan, X. Ma, *Appl. Surf. Sci.,* 356 (2015) 289-293.
27. T. Yin, R. Wu, Z. Leng, G. Du, X. Guo, M. Zhang, J. Zhang, *Surf. Coat. Technol*., 225 (2013) 119-125.
28. J. Tang, K. Azumi, *Electrochim. Acta*, 56 (2011) 8776-8782.
29. C. Xie, H. Li, X. Zhou, C. Sun, *Surf. Coat. Technol*., 374 (2019) 797-806.
30. J. Chen, B. Ma, S. Feng, Y. Dai, G. Liu, H. Song, L. Jia, *Surf. Eng*., 35 (2019) 351-359.
31. Y. Bai, Z.H. Wang, X.B. Li, G.S. Huang, C.X. Li, Y. Li, *J. Alloys Compd*., 719 (2017) 194-202.
32. B.S. DeForce, T.J. Eden, J.K. Potter, J. Therm. *Spray Technol.,* 20 (2011) 1352-1358.
33. K. Spencer, D.M. Fabijanic, M.X. Zhang, *Surf. Coat. Technol*., 204 (2009) 336-344.
34. M.R. Elahi, M.H. Sohi, A. Safaei, *Appl. Surf. Sci*., 258 (2012) 5876-5880.
35. S. Peng, S.-K. Xie, F. Xiao, J.-T. Lu, *Corros. Sci*., 163 (2020) 108237.
36. D. Persson, D. Thierry, O. Karlsson, *Corros. Sci*., 126 (2017) 152-165.
37. A.R. Marder, The metallurgy of zinc-coated steel, *Prog. Mater. Sci*., 45 (2000) 191-271.
38. T.A. Vida, C. Brito, T.S. Lima, J.E. Spinelli, N. Cheung, A. Garcia, *Current applied physics*, 19 (2019) 582-598.
39. J. Huang, Y. Lai, H. Jin, H. Guo, F. Ai, Q. Xing, X. Yang, D.J. Ross, *J. Mater. Eng. Perform*., 29 (2020) 6484-6493.
40. D.-g. Li, Q. Wang, G.-j. Li, X. Lv, K. Nakajima, J.-c. He, *Materials Science and Engineering*: A, 495 (2008) 244-248.
41. Y. Su, X. Lin, M. Wang, W. Huang, *J. Mater. Sci.,* 56 (2021) 14314-14332.
42. M. Lotfpour, C. Dehghanian, M. Emamy, A. Bahmani, M. Malekan, A. Saadati, M. Taghizadeh, M. Shokouhimehr, *J. Magnesium Alloys*, 9 (2021) 2078-2096.
43. Y. Ma, H. Xiong, B. Chen, *Corros. Sci.,* 191 (2021) 109759.
44. T. Zhang, G. Meng, Y. Shao, Z. Cui, F. Wang, *Corros. Sci.,* 53 (2011) 2934-2942